CHAPTER 5

Magnetic and transport properties of conjugated and cumulated molecules: the π-system enlightens part of the story

Abstract

In the fifth chapter we have investigated the intramolecular magnetic exchange coupling constants (J) for a series of nitronyl nitroxide diradicals connected by a range of linear conjugated and cumulene couplers focusing on the unusual π-interaction properties within the couplers. Distance between radical centers, spin density within the couplers, as well as the dihedral angles between the radical centers and the plane of the coupler influence the strength of magnetic coupling. We also establish that with the increase in length of the coupler, the strength of magnetic interaction in conjugated and cumulated systems varies in a different way. Transport calculations show that with the increase in chain length, diradicals based on cumulene containing even number of carbon atoms act as better conductors than cumulenes with odd number of carbon atoms. It is also observed that with the increase in the length of the conjugated coupler based diradicals, transmission does not vary in a sequential way.

5.1 Introduction

The magnetic interactions of organic radicals[1] and methods of controlling their magnetic properties have been widely investigated for their potential applications in the field of magnetism,[2] superconductivity,[3,4] photomagnetism,[5,6] spintronics[7,8] including their use in spin field effect transistors, magnetic semiconductors, spin-polarized light-emitting diodes, spin valves, and so on.[9-12] On the other hand, tunable molecular wires that reconcile electronic communication,[13] energy transfer,[14] electron transfer,[15] charge transport [16] etc. have been sparkles in the eye of theoreticians and experimentalists.[17]

Spintronic elements whose transport properties are governed by antiferromagnetic interactions are also known.[18] Much efforts have been given over the past decades to the design and synthesis of π-conjugated molecular wires[19] (containing delocalized electrons) and it is a persistent challenge in molecular electronics to control the conductance and current flow through such systems. Getting high conductance is also of interest in the distance-dependent attenuation of electron transfer and transport.[20-22]

Among all carbon nanostructures, linear chains of carbon atoms have been predicted to have excellent properties for various transport related applications.[23-25] It is found that chains containing sp-hybridized carbon atoms are fascinating due to their unique linear structure and interesting physical properties.[26-29] Recently allenes have acquired major attraction as their reactivity and selectivity can be simply tuned by varying their electronic and steric effects with appropriate substituents.[30,31] Zhang et al. have shown that cumulenes act as semiconductors and polyynes as metallic monatomic chains by their rigidity, these properties make them promising for applications in nanotechnology.[32] Cumulenes and their substituted counterparts have also been used as elements for nonlinear optics, molecular sensors,[33] molecular machines (nanomechanics),[34] molecular wires (nano-electronics, which is an emerging field in structural chemistry). Skibar et al.[35] and Januszewski et al.[36,37] have synthesized and predicted the properties of long cumulene systems.

The magnetic interaction between two radical centers generally depends on the distance and the nature of the couplers.[38-42] The π-interaction as well as the spin-polarization through the coupler play a major role in controlling the magnitude and sign of the coupling constant.[43]An estimation of the exchange coupling constant is necessary before synthesizing a successful organic magnetic material based on organic diradicals. There are many systematic studies on the intramolecular magnetic coupling constants for organic diradicals linking with various couplers.[44-54] Recently we have studied the anomalous magnetic property of diradicals based on chiral allene and cumulene coupler (containing odd number of carbon atoms) where the π-orbitals at both end of the coupler are perpendicular to each other and may be used as building blocks for chiral magnets.[55] For cumulenes containing even number of carbon atoms,

the π-orbitals at both end of the cumulene chain are parallel to each other and hence have different electronic structure compared to that of odd cumulenes. On the other hand, conjugated systems have alternating double bonds. Therefore, as a continuation of our previous work,[55] we are motivated to investigate the effect of unusual π-interaction of cumulene based diradicals containing even number of carbon atoms as well as diradicals based on conjugated systems (shown in Figure 5.1) on the magnetic properties, as this will provide a completeness to this study. We use nitronyl nitroxide radicals as radical sources where the unpaired spin comes from the -NO group of the nitronyl nitroxide moiety.[56] In addition to that; we also study the coherent electronic transport characteristics of cumulene based diradicals (with both the odd and even number of carbon atoms) and the conjugated couplers.

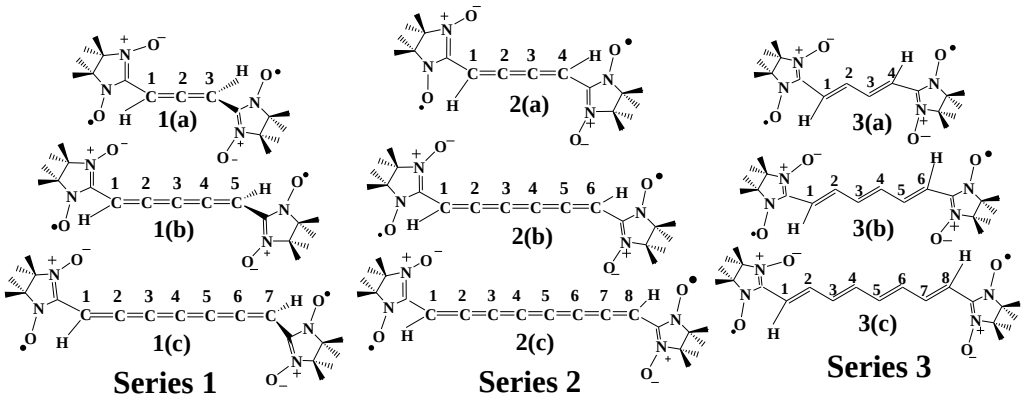

Figure 5.1 Designed diradicals based on allene, cumulene and the conjugated couplers. Series 1 represents the allene and cumulene based diradicals containing odd number of carbon atoms, Series 2 represents cumulene based diradicals containing even number of carbon atoms and Series 3 represents the diradical based on conjugated systems.

5.2 Theoretical background and computational strategy

The magnetic exchange interaction between two magnetic sites 1 and 2 is normally expressed by the Heisenberg spin Hamiltonian $\hat{H} = -2J\hat{S}_1 \bullet \hat{S}_2$, where $\hat{S}_1$ and $\hat{S}_2$ are the respective spin angular momentum operators and *J* is the effective exchange coupling constant between two magnetic sites. Positive sign of *J* means the coupling is ferromagnetic and the high-spin state is the lower energy state. A negative value of *J* is representative of antiferromagnetic interaction in the diradical and a low-spin state is the ground state. For a diradical having a single unpaired electron on each site, *J* can be represented as $E_{(S=1)} - E_{(S=0)} = -2J$.

Multi-configuration approaches are appropriate to describe pure spin states in a proper manner; but these methods are resource intensive and not used in this work. To circumvent this issue, broken symmetry (BS) approach proposed by Noodleman et al.[57-60] in DFT framework is a more useful alternative to evaluate *J* that can ultimately lead to an estimation of the energy of diradical singlets. The limiting form of the BS state is a weighted average of the singlet and the triplet, and has M_S =0. The ideal triplet (*T*) state has an $\langle S^2 \rangle$ = 2, whereas $\langle S^2 \rangle$= 1 in the ideal BS state and that results $E(\mathrm{BS}) - E(\mathrm{T}) = J$. However in actual calculation approximate $\langle S^2 \rangle$ values are obtained, and hence BS solution is often found to be spin contaminated. Therefore, a correction is needed to calculate the coupling constant. The spin projected formula given by Yamaguchi[61-64] for the estimation of magnetic exchange coupling constant (*J*) is capable of taking such spin contamination into account and applicable for both low and high overlaps between magnetic orbitals, that can be written as $J = (E_{BS} - E_{HS}) \Big/ \left(\left\langle S^2 \right\rangle_{HS} - \left\langle S^2 \right\rangle_{BS} \right)$ where E_{BS}, E_{HS} and $\langle S^2 \rangle_{BS}$, $\langle S^2 \rangle_{HS}$ are the energy and average spin square values for corresponding BS and high-spin states.

All calculations related to magnetic properties have been done by Gaussian09 package.[65] The popular B3LYP exchange–correlation potential was used in combination with the 6-311++G(d,p) basis set within the unrestricted formalism for all geometry optimizations. Frequency calculation gives positive values for all these systems which confirm that the geometries are in local minima. To obtain open shell broken symmetry (BS) singlet solution "guess=(read,mix)" keyword is used for mixing of the HOMO and the LUMO. The magnetic exchange coupling constant (*J*) value for each molecule has been estimated from the energies of triplet and BS states at the same level of theory using the spin projected formula given by Yamaguchi.

In the coherent tunnelling regime the finite bias current ($I_s(V)$) conduction of electron spins through a gold-molecule-gold junction can be calculated by the following equation:

$$I_s(V) = \frac{e}{h} \int_{E_F - \frac{eV}{2}}^{E_F + \frac{eV}{2}} dE T_S(E,V) \qquad (1)$$

where *V* is the finite bias voltage, E_F is the Fermi energy, *E* is the energy and $T_S(E,V)$ is the transmission function. In the Landauer–Imry–Büttiker approximation,[66] the zero voltage conductance i.e., $(dI/dV)_{V=0}$ is proportional to $T(E_F)$. Therefore, it is reasonable to take integration over $E_F - \frac{eV}{2}$ to $E_F + \frac{eV}{2}$. The T_s can be calculated from the retarded ($\Gamma_{L/R,s}$) and advanced ($G_{C,sr/a}$) Green's function of the electrode-molecule-electrode system as

$$T_S(E,V) = tr\left(\Gamma_{R,s} G^r_{L,s} \Gamma_{L,s} G^a_{C,s}\right) \qquad (2)$$

The detailed theoretical approach we use here can be found in reference 67 and 68.

In order to obtain the transport properties of all the designed systems, instead of simply considering the prototypical diradical based on cumulene and conjugated couplers, we add polyacetylene chain (spacer groups, containing 4 carbon atoms), ensuring that there is no considerable interaction between the electrodes and any atom of the radical sites. The dithiol (obtained by replacing two end hydrogen atoms of polyyne chain by –SH group) molecule has been optimized and then the hydrogen atoms are stripped off and the resulting neutral dithiolate is placed between two electrodes (shown in Figure 5.2). Each electrode consists of nine gold atoms that are organized as a six-atom triangular fcc-gold (111)-surface connected to the molecule, with a second layer having three gold atoms. The bond length between sulfur and Au (111) surface has been chosen to be 2.48 Å and Au-Au distances of 2.88 Å as in extended gold crystals. Fock and overlap matrices required for the transport calculations are achieved by single point calculation in Gaussian09 program package.[65] For the transport calculation we employ B3LYP functional and the LANL2DZ basis set to avoid ghost transmission.[67] Basis sets of triple-zeta quality or higher sometime gives an artificially high transmission and possibly may give wrong conclusions about chemical trends. In such cases, transport persists when molecular atoms are substituted by basis functions alone (called "ghost atoms"). It is tested that the basis set of double zeta quality without polarization functions (e.g. Lanl2dz) gives negligible ghost transmission. This observation has been systematically studied by Herrmann and co-workers given in reference 67.

In order to obtain the transport properties, the designed systems have been divided into three sub systems: gold-cluster–dithiolate–gold-cluster as illustrated in Figure 5.2. We have calculated the transmission property using ARTAIOS code developed by Herrmann et al.[67-68]

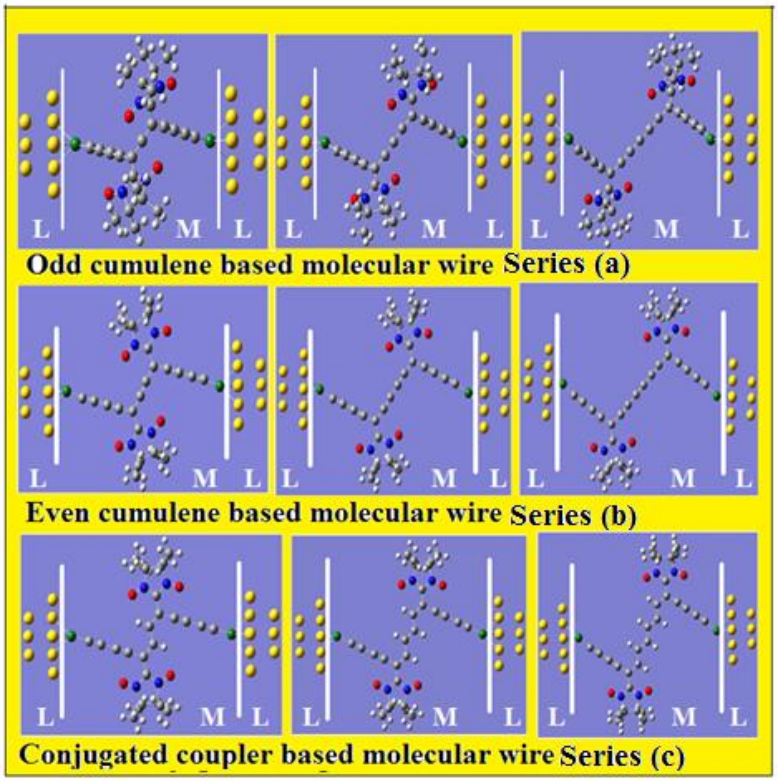

Figure 5.2 Designed diradical based systems on which transport calculations have been carried out (L stands for lead and M stands for molecule, the grey, white, red, blue, yellow and green colors represent carbon, hydrogen, oxygen, nitrogen, gold and sulfur atoms respectively). Series (a) represents odd cumulene based molecular wires, Series (b) represents even cumulene based molecular wires and Series (c) represents conjugated coupler based molecular wires.

5.3 Results and discussion

5.3.1 Magnetic exchange coupling constant

The calculation of *J* yields ferromagnetic interaction for linkers with an odd number of carbon atoms,[55] while antiferromagnetic coupling is predicted for diradicals connected by linkers with an even number of carbon atoms shown in Figure 5.3 (using B3LYP/6-311++G(d,p)). It is found that the increase in number of carbon atoms from odd cumulene connector to even cumulene connector causes a great contrast in magnitude as well as the change in sign of the magnetic exchange coupling constant values. It is also observed that with the increase in the number of carbon atoms of the coupler, the magnitude of *J* increases for both the series of odd and even cumulene based diradicals [the increase of *J* through the odd cumulene based diradical series is almost twice from 1(a) to 1(b) and from 1(b) to 1(c)],[55] while for conjugated couplers, the magnitude of *J* value decreases gradually. Therefore

cumulenes with even number of carbon atoms show an increase in coupling constant value with the increase in the distance between two radical centers; though opposite result is normally expected keeping parity with the conjugated systems. Thus together with the previous work[55] it provides completeness to this particular study. Therefore, it can be argued that there must be a major contribution of the π-interaction of the couplers in magnetic exchange pathways and this observation demands a detailed investigation of electronic structure of these couplers.

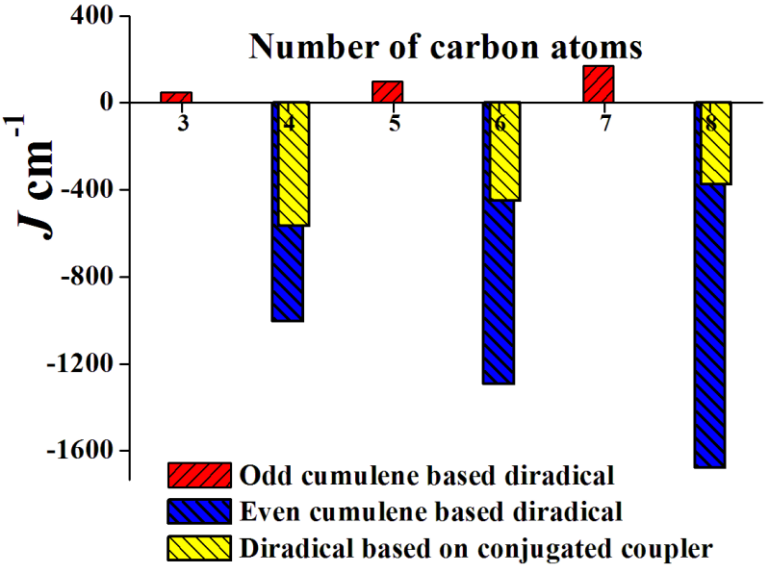

Figure 5.3 Plot of magnetic exchange coupling constant J (in cm^{-1}) vs. number of carbon atoms within the coupler (using B3LYP/6-311++G(d,p)). Red color represents the coupling constant for odd cumulene based diradical (series 1), blue color represents even cumulene based diradical (series 2), and yellow color represents diradical based on conjugated coupler (series 3).

B3LYP is a well-tested and widely used functional but it lacks dispersion correction and long range correction. Therefore, in addition to B3LYP, we compute the magnetic exchange coupling constant of our designed systems with dispersion corrected B3LYP (B3LYP-D) and to include long range correction we use CAM-B3LYP and the results are given in Table 5.1, Table 5.2 and Table 5.3. We found that there is no qualitative change of the magnetic exchange coupling constant due to dispersion correction and long range correction in the functional. All the functionals give qualitatively consistent results except CAM-B3LYP functional gives average spin square value far from 1 to the BS solution. Considering all these facts, we stick to the B3LYP functional for rest of the calculations.

Table 5.1 The energy (a.u.),$\langle S^2 \rangle$ and magnetic exchange coupling constant (J in cm^{-1}) of the odd cumulene based diradicals (taken from reference 55).

Diradicals			Triplet	BS	*J*
B3LYP/ 6-311++G(d,p)	1(a)	E(a.u.)	-1183.41922	-1183.41900	47.66
		$\langle S^2 \rangle$	2.136	1.123	
	1(b)	E	-1259.59164	-1259.59117	99.09
		$\langle S^2 \rangle$	2.207	1.166	
	1(c)	E(a.u.)	-1335.76802	-1335.76716	171.28
		$\langle S^2 \rangle$	2.319	1.217	
B3LYP-D/ 6-311++G(d,p)	1(a)	E(a.u.)	-1183.48377	-1183.48355	48.05
		$\langle S^2 \rangle$	2.136	1.124	
	1(b)	E	-1259.65614	-1259.65566	101.73
		$\langle S^2 \rangle$	2.208	1.169	
	1(c)	E(a.u.)	-1335.83327	-1335.83239	176.10
		$\langle S^2 \rangle$	2.320	1.223	
CAM-B3LYP/ 6-311++G(d,p)	1(a)	E(a.u.)	-1182.84108	-1182.84058	106.44
		$\langle S^2 \rangle$	2.261	1.235	
	1(b)	E	-1258.96336	-1258.96194	279.92
		$\langle S^2 \rangle$	2.453	1.340	
	1(c)	E(a.u.)	-1335.09014	-1335.08668	587.94
		$\langle S^2 \rangle$	2.824	1.529	

Table 5.2 The energy (a.u.),$\langle S^2 \rangle$ and magnetic exchange coupling constant (J in cm^{-1}) of the even cumulene based diradicals.

Diradicals			Triplet	BS	*J*
B3LYP/ 6-311++G(d,p)	2(a)	E(a.u.)	-1221.50674	-1221.51048	-1003.86
		$\langle S^2 \rangle$	2.119	1.302	
	2(b)	E	-1297.67951	-1297.68382	-1291.24
		$\langle S^2 \rangle$	2.137	1.404	
	2(c)	E(a.u.)	-1373.85534	-1373.86026	-1679.34
		$\langle S^2 \rangle$	2.156	1.513	
B3LYP-D/ 6-311++G(d,p)	2(a)	E(a.u.)	-1221.56528	-1221.56946	-1172.14
		$\langle S^2 \rangle$	2.118	1.335	
	2(b)	E(a.u.)	-1297.74438	-1297.74873	-1302.45
		$\langle S^2 \rangle$	2.137	1.406	
	2(c)	E(a.u.)	-1373.92099	-1373.92594	-1695.14
		$\langle S^2 \rangle$	2.156	1.515	
CAM-B3LYP/ 6-311++G(d,p)	2(a)	E(a.u.)	-1220.89356	-1220.90261	-3256.97
		$\langle S^2 \rangle$	2.226	1.616	
	2(b)	E(a.u.)	-1297.02294	-1297.03155	-3429.87
		$\langle S^2 \rangle$	2.253	1.703	
	2(c)	E(a.u.)	-1373.14718	-1373.15792	-6158.36
		$\langle S^2 \rangle$	2.296	1.913	

Table 5.3 The energy (a.u.),$\langle S^2 \rangle$ and magnetic exchange coupling constant (J in cm^{-1}) of the diradical based on conjugated systems.

Diradicals			Triplet	BS	*J*
B3LYP/ 6-311++G(d,p)	3(a)	E(a.u.)	-1222.77595	-1222.77989	-565.03
		$\langle S^2 \rangle$	2.117	1.225	
	3(b)	E	-1300.20673	-1300.20855	-450.12
		$\langle S^2 \rangle$	2.133	1.245	
	3(c)	E(a.u.)	-1377.63530	-1377.63681	-373.53
		$\langle S^2 \rangle$	2.147	1.264	
B3LYP-D/ 6-311++G(d,p)	3(a)	E(a.u.)	-1222.84466	-1222.84684	-536.49
		$\langle S^2 \rangle$	2.117	1.227	
	3(b)	E(a.u.)	-1300.27678	-1300.27863	-456.71
		$\langle S^2 \rangle$	2.133	1.247	
	3(c)	E(a.u.)	-1377.70835	-1377.70988	-379.74
		$\langle S^2 \rangle$	2.148	1.266	
CAM-B3LYP/ 6-311++G(d,p)	3(a)	E(a.u.)	-1222.17266	-1222.17652	-1029.03
		$\langle S^2 \rangle$	2.217	1.393	
	3(b)	E(a.u.)	-1299.55258	-1299.55564	-828.31
		$\langle S^2 \rangle$	2.249	1.439	
	3(c)	E(a.u.)	-1376.93172	-1376.93426	-699.12
		$\langle S^2 \rangle$	2.280	1.483	

Singlet and Triplet weightings[69] Considering a general BS state which is a nearly equal superposition of singlet (S) and triplet (T) states. We can write

$$\psi_{BS} = m\,\psi_S^{BS} + n\,\psi_T^{BS}$$

Where $m^2 \approx n^2 \approx 1/2$, $m^2 + n^2 = 1$ and $n^2 = 0.5\,\langle S^2 \rangle_{BS}$

Therefore $m^2 = 1 - 0.5\langle S^2 \rangle_{BS.}$ The net weights of singlet and triplet components in the BS solution are given in Table 5.4, Table 5.5, and Table 5.6.

Table 5.4 Percent Net Weight of Triplet and Singlet Components in the Computed BS Solution (B3LYP/6-311++G(d,p)). $\langle S^2 \rangle_{BS}$ values of series 1 diradicals are taken from ref 55.

System	singlet % weight ($100m^2$)	triplet % weight ($100n^2$)
1(a)	43.85	56.15
1(b)	41.70	58.30
1(c)	39.15	60.85
2(a)	34.90	65.10
2(b)	29.80	70.20
2(c)	24.35	75.65
3(a)	38.75	61.25
3(b)	37.75	62.25
3(c)	36.80	63.20

Table 5.5 Percent Net Weight of Triplet and Singlet Components in the Computed BS Solution (B3LYP-D/6-311++G(d,p)).

System	singlet % weight ($100m^2$)	triplet % weight ($100n^2$)
1(a)	43.80	56.20
1(b)	41.55	58.45
1(c)	38.85	61.15
2(a)	33.25	66.75
2(b)	29.70	70.30
2(c)	24.25	75.75
3(a)	38.65	61.35
3(b)	37.65	62.35
3(c)	36.70	63.30

Table 5.6 Percent Net Weight of Triplet and Singlet Components in the Computed BS Solution (CAM-B3LYP /6-311++G(d,p)).

System	singlet % weight ($100m^2$)	triplet % weight ($100n^2$)
1(a)	38.25	61.75
1(b)	33.00	67.00
1(c)	23.55	76.45
2(a)	19.20	80.80
2(b)	14.85	85.15
2(c)	4.35	95.65
3(a)	30.35	69.65
3(b)	28.05	71.95
3(c)	25.85	74.15

Factors affecting magnetic exchange coupling

The magnetic interaction depends on the distance *r* between the magnetic centers as *exp*(-*r*),[70] therefore for our designed systems one may expect a decrease in coupling constant value with the increase in the number of carbon atoms within the coupler (as the distance between radical centers also increases given in Table 5.7). But for odd-numbered cumulene series (1(a), 1(b), and 1(c)), the coupling constant is positive and increases in magnitude with the increase in number of carbon atoms in cumulene chain (shown in Figure 5.4). The relation is almost perfectly linear (R^2 =0.99, from regression analysis).

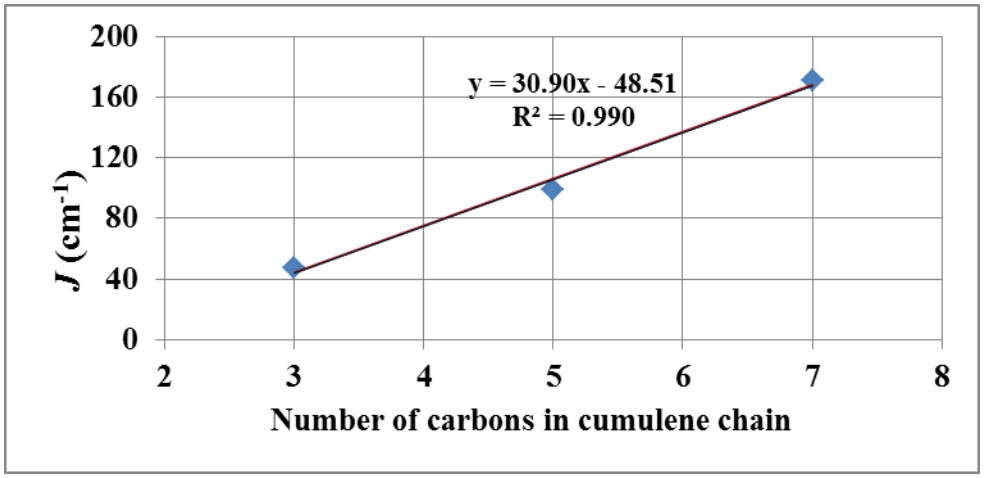

Figure 5.4 Plot of *J* (cm^{-1}) vs. number of carbon atoms in cumulene chain (regression analysis) for odd cumulene series (1(a), 1(b), and 1(c)) (using B3LYP/6-311++G(d,p)).

For even numbered cumulenes (2(a), (b), and (c)) the coupling constant also is linear with the increase in number of carbon atoms in cumulene chain (shown in Figure 5.5), but is negative, and larger in magnitude. The relation is almost perfectly linear (R^2 >0.99 from regression analysis).

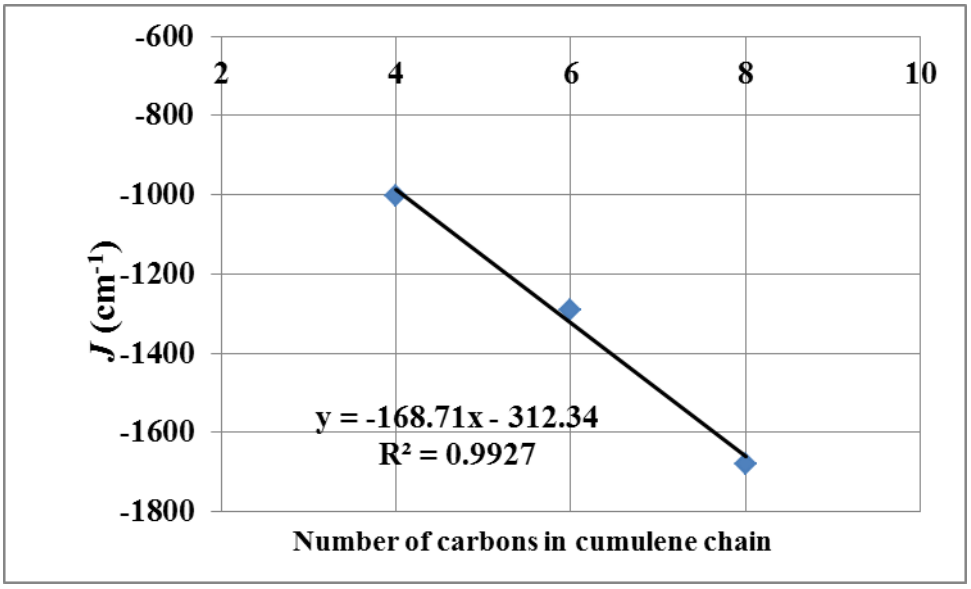

Figure 5.5 Plot of J (cm^{-1}) vs. number of carbon atoms in cumulene chain (regression analysis) for even cumulene series (2(a), (b), and (c)) (using B3LYP/6-311++G(d,p)).

Polo et al. have shown that the magnitude of J depends strongly on the planarity of the molecular structure of the diradical as more effective orbital overlap between the π-systems can thus be reached.[71] Shil et al. have also shown that when the coupler and the radical centers are in different planes, coupling between them decreases.[72] Therefore, there are certain factors (such as the distance between radical centers, spin polarization pathways, and the planarity of the molecular structure of the diradical), make it difficult to predict the values of J.

(i) Distance between radical centers *r* (in Å)

Table 5.7 Distance between radical centers r (in Å) (using B3LYP/6-311++G(d,p)).

System	*r* (in Å)	*J* (cm^{-1})	System	*r* (in Å)	*J* (cm^{-1})	System	*r* (in Å)	*J* (cm^{-1})
1(a)	4.256	47.66	2(a)	6.407	—1003.86	3(a)	6.989	—565.03
1(b)	5.790	99.09	2(b)	7.869	—1291.24	3(b)	9.263	—450.12
1(c)	7.873	171.28	2(c)	9.815	—1678.7	3(c)	11.391	—373.53

From the Table 5.7 it is clear that continuing from the smaller coupler to its higher homologues in each series, the distance between radical centers increases as expected. Therefore there should be a decrease in *J* values from smaller to the larger coupler as discussed earlier.[70] This trend is observed in the conjugated systems of series 3, but for cumulene couplers of series 1 and series 2, opposite result is found. This result clearly indicates that the magnitude of the coupling constant values not only depend on the distance between the radical centers but also on other factors which are discussed under subsequent points.

(ii) Spin density distribution on the coupler

The spin density of DFT based approach gives us an insight about the spin polarization mechanism for magnetic exchange coupling within the molecule. Hermann et al. have proposed that for cumulene systems (with even number of carbon centers), the spin delocalization onto the chain increases as the length of the chain gets longer.[73] From the spin density distribution plot of Figure 5.6 it is observed that for even cumulene based diradicals there is an accumulation of excess spin density on all the middle carbon atoms of the coupler i.e., along y and z direction collectively (represented by the red arrow). From Table 5.8 it is clear that the spin density on each carbon of the coupler and the average spin density increases with the increase in the length of the coupler. In our previous work we have shown that for odd cumulene based diradicals, a large accumulation of spin density within the coupler occurs due to the presence of two π-electrons at a time on each sp-carbon atom of the coupler,[55] and this also occurs for even cumulene based diradicals.

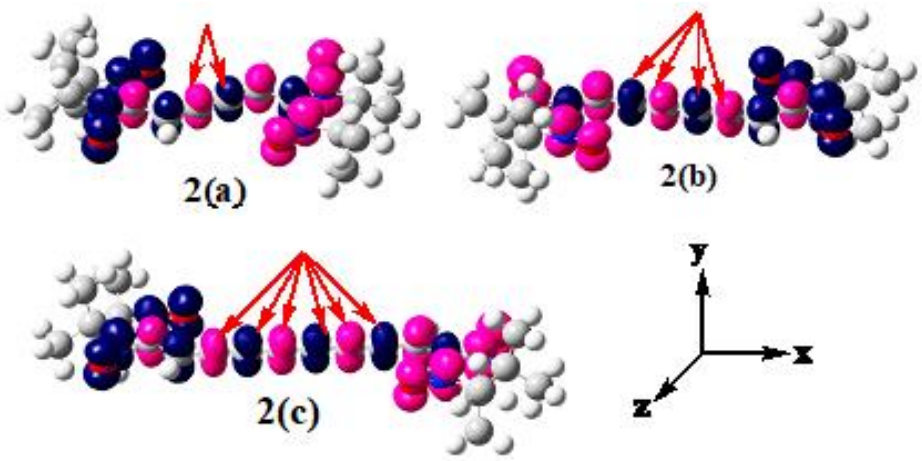

Figure 5.6 Spin density plot for the even cumulene based diradicals (series 2) in their BS states (B3LYP/6-311++G(d,p)) (iso value 0.004), magenta and blue colors represent the α and β spins respectively. Red arrow represents the carbons with excess spin density.

Table 5.8 Spin density distribution on each atom of the coupler of even cumulene-based diradicals in their BS state (B3LYP/6-311++G(d,p)).

System	Spin density on different atoms of coupler								Average spin density on each atom of the coupler
	C_1	C_2	C_3	C_4	C_5	C_6	C_7	C_8	
2(a)	0.2260	-0.2082	0.2082	-0.2260	-------	---------	--------	---------	0.2171
2(b)	0.2407	-0.2274	0.2484	-0.2484	0.2274	-0.2407	--------	---------	0.2388
2(c)	0.2630	-0.2510	0.2620	-0.2123	0.2123	-0.2619	0.2510	-0.2630	0.2471

But in case of conjugated systems spin density of the coupler is distributed in one direction only i.e., along y direction only (shown in Figure 5.7) and with the increase in length of the coupler, a decrease in average spin density is observed from Table 5.9. Therefore, spin density is one of the major factors that results the ultimate increases in *J* values for diradicals based on cumulene systems and decreases for diradicals based on conjugated couplers with the increase in number of carbon atoms of the coupler.

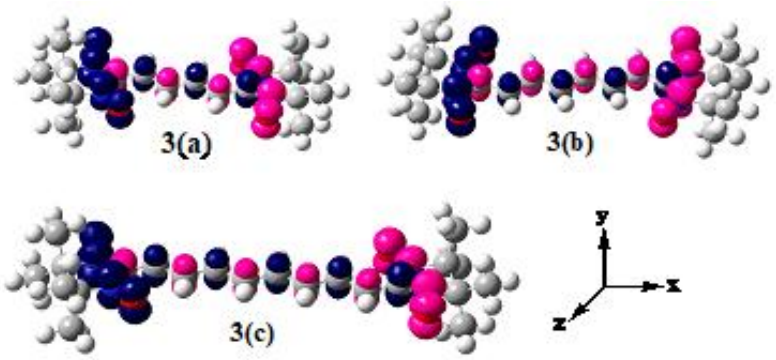

Figure 5.7 Spin density plot for the diradical based conjugated systems (series 3) in their BS states (B3LYP/6-311++G(d,p)) (iso value 0.004), magenta and blue colors represent the α and β spins respectively.

Table 5.9 Spin density distribution on each atom of the coupler of diradical based on conjugated systems in their BS state (B3LYP/6-311++G(d,p)).

System	Spin density on different atoms of coupler								Average spin density on each atom of the coupler
	C_1	C_2	C_3	C_4	C_5	C_6	C_7	C_8	
3(a)	0.1845	-0.1637	0.1637	-0.1845	--------	---------	--------	-------	0.1741
3(b)	0.1607	-0.1596	0.1342	-0.1342	0.1596	-0.1607	--------	-------	0.1515
3(c)	0.1704	-0.1639	0.1278	-0.1335	0.1335	-0.1278	0.1651	-0.1706	0.1491

(iii) Dihedral angle

The cumulenes – (C_n) – (where n either even or odd number of carbon atoms) have two orthogonal π-systems, while the conjugated systems – $(HC{=}CH)_k$ – have only one π-orbital (with k taking values 2, 3, and 4). For cumulene systems with nitronyl nitroxide end groups, the two types of perpendicular π-interactions are represented by red and blue arrows (in Figure 5.8(a) and (b)), whereas for conjugated systems only one π-interaction is shown by blue arrow (in Figure 5.8(c)). In odd cumulene based diradicals (Figure 5.8(a)), the extent of π-interaction between cumulene chain and the radical end groups are lower compared to the π-interaction in even cumulene based diradicals (Figure 5.8(b)). This is because for odd cumulenes, each type of π-interaction (represented by red/blue arrow in Figure 5.8(a)) can conjugate with one radical site at a time but not with the both radical end groups (as the two radical centers are not in same plane). But for even cumulene systems (Figure 5.8(b)), among the two π -interactions of the cumulene chain, one π -system (the π-interaction is represented by blue arrow) extends the length of the cumulene skeleton and can conjugate with both sides of end groups (Figure 5.8(b), where the two radical centers are in same plane).[36] Therefore for odd cumulene based diradicals, the perpendicular plane between two radical centers causes a small magnitude of coupling constant, but for even cumulene based diradicals, the planarity of two radical centers causes large magnitude of coupling constant values.

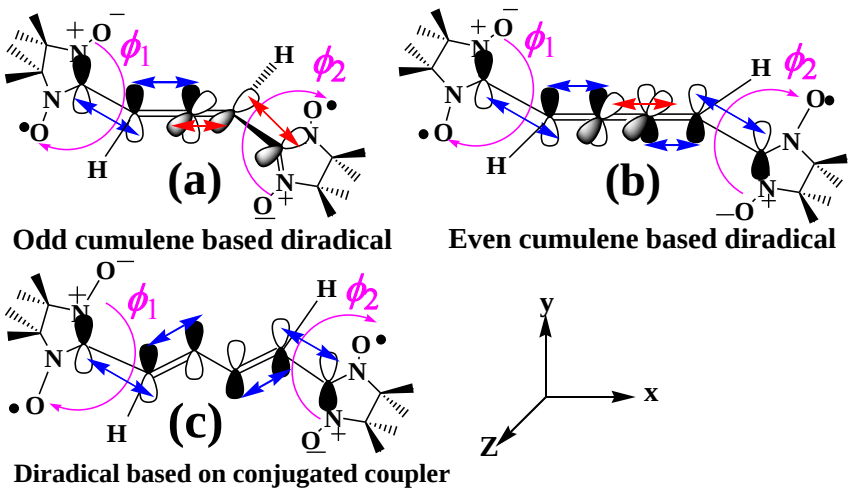

Figure 5.8 π-interaction of diradical based on cumulene and conjugated couplers. $\varphi_1$and φ_2 denote the dihedral angle between the plane of coupler and that of the nitronyl nitroxide radicals (blue arrow represents one π-interaction (i.e, overlap between p_y-p_y orbitals) and red arrow represents another π-interaction (i.e, p_z-p_z orbitals)). We have taken a representative figure from each series. (a) represents π-interaction of odd cumulene based diradicals, (b) represents π-interaction of even cumulene based diradicals, (c) represents π-interaction of diradical based on conjugated systems.

For even cumulene couplers, as the distance between radical sites increases the interaction may be expected to decline. However the increase in average spin density within the cumulene connector enhances the interaction. The net effect is small. For diradical based on conjugated couplers, there is only one π-interaction that can conjugate with both sets of end groups (shown in Figure 5.8(c)), but the increase in distance as well as the decrease in spin density within the coupler cause overall decrease in *J* value with increase in chain length of the coupler. Therefore, as a whole the π-interaction is the enlightening factor that controls the magnetic property of our designed systems.

5.3.2 Coherent electron transport through diradicals

Cumulene wires are known to be the potential candidates in nano-electronic applications.[74] Prasongkit et al. have theoretically studied the conductivity of cumulene based molecular wires and showed that all cumulenes yield higher conductance compared to other conjugated polymers, and for the odd-cumulene wires the conductance is still higher than that of even-cumulene wires as well as polyynes.[74] They also showed that the conductance of odd-cumulenes do not exhibit any marked dependence on the molecular length. However, Kondo et al. show an exponential decrease of transmission for oligo (p-phenylene) dithiolate wires with the increase in distance between two leads.[75] Apart from polyyne and cumulene systems, the polyene systems have a series of alternating single and double bonds through which transmission is possible.[76]

Magnetic molecules have wide applications in the field of spintronics.[77] In recent times organic radicals capable of constructing the spintronic devices like spin valves, spin filters, etc. are reported.[78] In order to design a diradical based electronic device it is important to understand the transport properties of the diradicals. Though much study has been made over the conductivity of cumulenes, in this section we try to understand the qualitative trend of transport property of the chiral cumulene based diradicals from our previous work[55] and the diradicals based on achiral cumulene and conjugated systems studied here. Schematic representations of the systems on which the transport property have been studied are given in Figure 5.9. Our comparison is based on the relative positions of transmission spectra with respect to each other, rather than on their absolute positions with respect to Fermi level of gold cluster. Therefore the addition of polyacetylene chain (spacer groups, containing 4 carbon atoms) at both ends of the cumulene and conjugated systems does not affect the transport property of the molecules under investigation because the acetylenic chains are conducting (also the relative positions of transmission spectra is not affected by the atom number of the electrode).

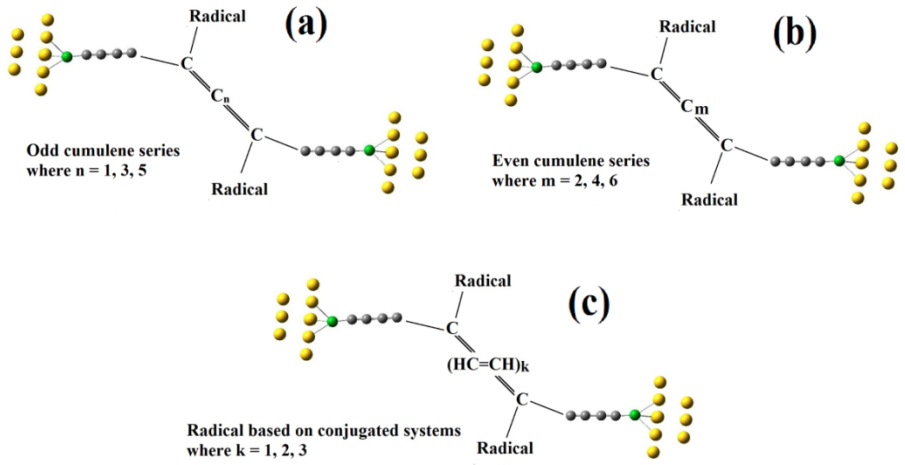

Figure 5.9 Schematic representation for the radical based systems on which the transport property have been studied.

For our designed systems (in Figure 5.9), the zero bias transmission spectra of the diradicals are given in Figure 5.10 (for α spin only). Usually the Fermi energy of bulk gold (−5.5 eV) is assumed,[79] but a Fermi energy of −5.0 eV is taken from DFT calculations.[80] For our calculation the Fermi energy is chosen to be −5.0 eV and marked with a dashed line in Figure 5.10 (therefore, when we compare the transmission spectra of our designed molecules, the shift in Fermi energy should be same for all the molecules with respect to Fermi level of gold cluster (-5 eV) and thus not affect qualitative comparisons based on the relative positions of transmission spectra of all the molecules with respect to each other). It is clear from Figure 5.10 that with the increase in length of the odd cumulene chains from [3]- to [5]-cumulene based diradicals and from [5]- to [7]- cumulene based diradicals (the number within the bracket represents the number of carbon atoms of the couplers within the two radical centers) the transmission decreases at the Fermi level (Figure 5.10(a)), but for even cumulene based diradicals from [4]- to [6]-cumulenes, transmission increases and after that (from [6]- to[8]-cumulene based diradicals) transmission value remains almost constant at the Fermi level (Figure 5.10(b)). Therefore, diradicals based on odd and even cumulene couplers show different characteristics of transmission. Moreover, Prasongkit et al. have shown that cumulene wire with odd number of carbon atoms gives higher transmission than that of the even one,[74] results from the high density of states of odd cumulene chains in lowest unoccupied molecular orbital levels that spans the Fermi level of the electrodes. But our calculation of cumulene based diradical shows the opposite trend (i. e., with the increase in length of the cumulene chain, even cumulene based diradicals have higher transmission compared to that of odd cumulene based diradicals). This is possibly due to the addition of radical within the cumulene systems. On the other hand transmission remains almost constant for diradical based on conjugated systems at the Fermi level marked with a dashed line at −5.0 eV (Figure 5.10(c)). For all of our designed systems, there is no difference

between α (in Figure 5.10) and β spin transmission (in Figure 5.11); therefore they have no spin filtering ability.

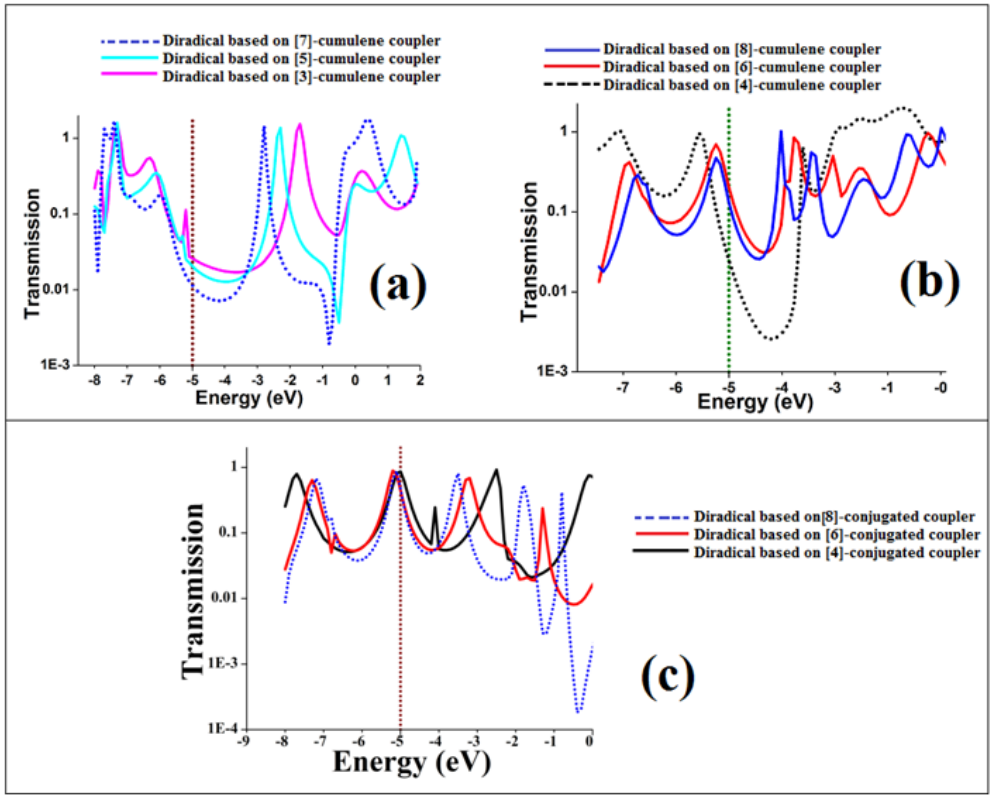

Figure 5.10 Transmission spectra of all the designed diradical based molecular wires (for α spin). (The transmission is expressed using a log scale). (a) represents the transmission spectra of odd cumulene based diradicals, (b) represents the transmission spectra of even cumulene based diradicals, (c) represents the transmission spectra of diradical based on conjugated systems.

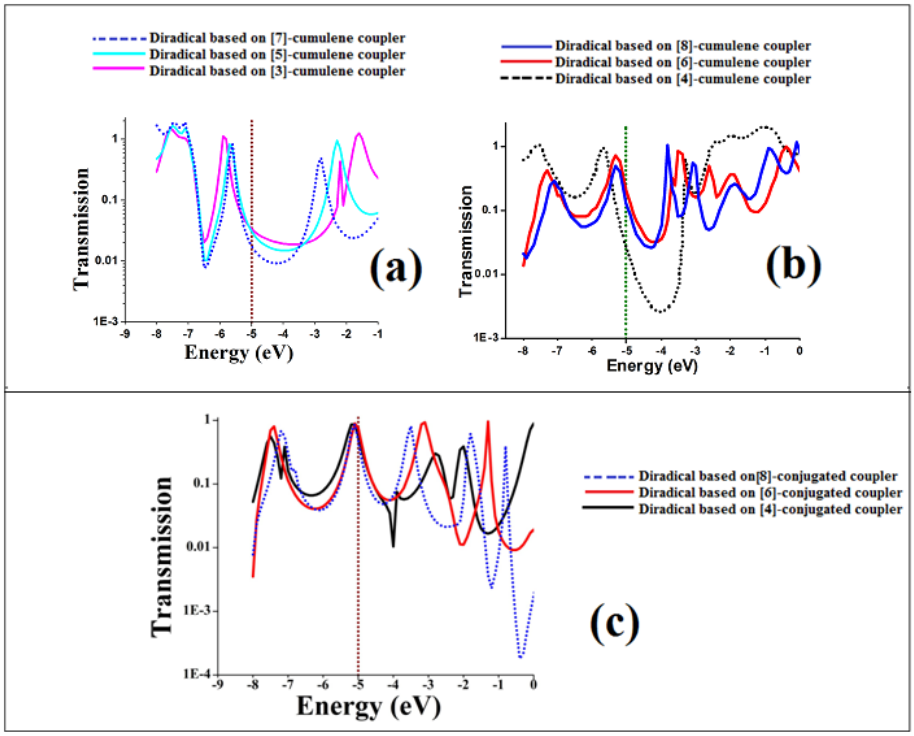

Figure 5.11 Transmission spectra of all the designed diradical based molecular wires (for β spin). (The transmission is expressed using a log scale). (a) represents the transmission spectra of odd cumulene based diradicals, (b) represents the transmission spectra of even cumulene based diradicals, (c) represents the transmission spectra of diradicals based on conjugated systems.

In order to understand the role of radical substitution on the transport property qualitatively, we have calculated the zero bias transmission spectra of cumulene and conjugated systems without radical centers shown in Figure 5.12.

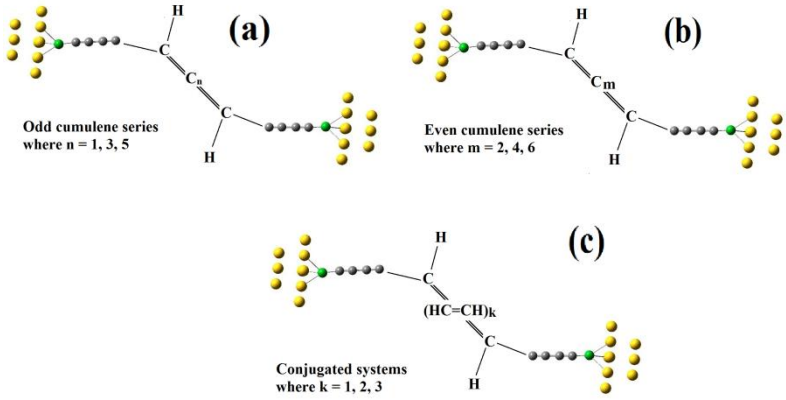

Figure 5.12 Schematic representations for the systems without radical centers on which the transport property have been studied.

For our designed systems without radical centers (in Figure 5.12), the zero bias transmission spectra are given in Figure 5.13.

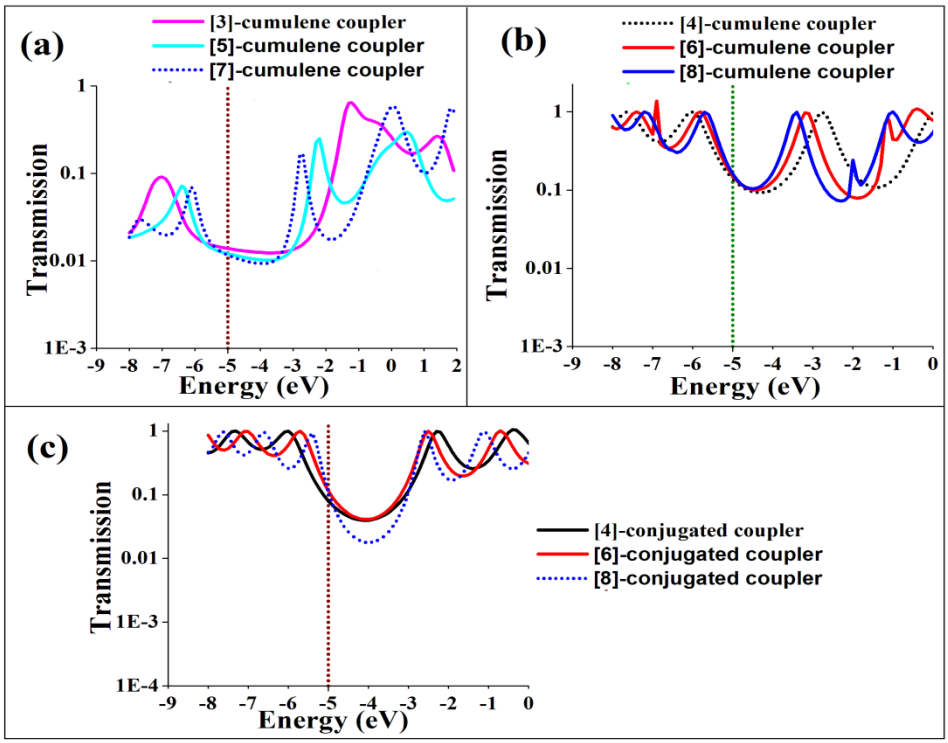

Figure 5.13 Transmission spectra of all the designed molecular wires without radical centers. (The transmission is expressed using a log scale). (a) represents transmission spectra of bare odd cumulene systems, (b) represents transmission spectra of bare even cumulene systems, and (c) represents transmission spectra of bare conjugated systems.

When we compare the results of diradical based systems (Figure 5.10(a) and Figure 5.10(b)) with that of bare systems (Figure 5.13(a) and Figure 5.13(b)); it is observed that, there is a variation in transmission with the increase in length of the odd and even cumulene based diradicals (in Figure 5.10(a) and Figure 5.10(b)), but for systems without radical centers (Figure 5.13(a), Figure 5.13(b)), the transmission remains constant at the Fermi level. Comparing the transmission value for diradicals based on conjugated systems with that of bare systems, it is found that for each set of molecules there is no variation of transmission values with the increase in chain length of the coupler. However, a higher transmission value is observed in case of radical based systems (Figure 5.10(c)) compared to bare systems (Figure 5.13(c)) at the Fermi level marked with a dashed line at −5.0 eV. Therefore, there is a contribution of radical substitution on the transport property.

Factors affecting transmission in radical substituted systems

(i) HOMO-LUMO energy gap

It is well known that the highest occupied molecular orbital (HOMO) and the lowest unoccupied molecular orbital (LUMO) play central roles for the transport properties[81-85] and the Fermi levels reside somewhere in between the HOMO and the LUMO. Schlicke et al. have proposed that if two radical centers are perpendicular to each other and also to the coupler, there is a loss of conjugation in between them, and that is reflected with an increase of the HOMO–LUMO gap, and further contributes to the low conductance.[86] Proppe et al. have suggested that in case of polyene systems the transmission increases at the Fermi level if there is a closer proximity of the HOMO energy and the Fermi energy.[87] Choi et al. showed that the molecular orbitals of a molecule with electrode atoms as well as without electrode atoms have similar orbital characteristics.[88] Therefore the transmission properties of a molecule between two electrodes can be manipulated by using our designed diradical systems (in Figure 5.1) without the gold electrodes. Hermann et al. also have shown that for cumulene based systems containing even number of carbon centers, the α-HOMO – α-LUMO gaps decreases with the increase in carbon chain length.[89] For our designed systems the frontier orbital energy are shown in Table 5.10 and Table 5.11. It is evident from these tables that, with the increase in the number of carbon atoms of the couplers in each series, frontier orbital energy splitting decreases gradually. Therefore an increase in transmission with the increase in number of carbon atoms in each series is expected. But from the transmission curve (Figure 5.10) it is clear that although the transmission characteristics show a predictable result to some extent for diradical based on even cumulene series, for diradical based on odd cumulenes and diradical based on conjugated systems the scenario is different. Hence, there must be some other factors guiding the situation.

Table 5.10 Energy (in eV) of $(HOMO-2)_\alpha$, $(HOMO-1)_\alpha$, $(HOMO)_\alpha$ and $(LUMO)_\alpha$ and Energy difference between $HOMO_\alpha$–$LUMO_\alpha$ (ΔE_{HL} in eV) for diradical based on odd cumulenes (B3LYP/6-311++G(d,p)) (taken from reference 55).

Systems	$(E_{HOMO-2})_\alpha$	$(E_{HOMO-1})_\alpha$	$(E_{HOMO})_\alpha$	$(E_{LUMO})_\alpha$	ΔE_{HL}
1(a)	-6.89275	-5.29989	-5.29309	-1.58143	3.71
1(b)	-6.54971	-5.39002	-5.38653	-2.36083	3.03
1(c)	-6.29637	-5.47614	-5.47329	-2.83002	2.64

Table 5.11 Energy (in eV) of $(HOMO-1)_{\alpha}$, $(HOMO)_{\beta}$, $(HOMO)_{\alpha}$ and $(LUMO)_{\alpha}$ and Energy difference between $HOMO_{\alpha}$–$LUMO_{\alpha}$ (ΔE_{HL} in eV) for diradical based on even cumulene and conjugated couplers (B3LYP/6-311++G(d,p)).

Systems	$(E_{HOMO-1})_{\alpha}$	$(E_{HOMO})_{\alpha}$	$(E_{HOMO})_{\beta}$	$(E_{LUMO})_{\alpha}$	ΔE_{HL}
2(a)	-5.98562	-5.43414	-5.43414	-2.71938	2.71
2(b)	-5.90437	-5.51172	-5.51172	-3.06425	2.45
2(c)	-5.85536	-5.57901	-5.57901	-3.29603	2.28
3(a)	-5.92453	-5.39471	-5.39471	-2.40915	2.99
3(b)	-5.71577	-5.38513	-5.38511	-2.56017	2.82
3(c)	-5.54832	-5.36897	-5.37308	-2.66809	2.70

(ii) Distance between leads (considering the distance between sulfur atoms)

In order to study the transmission characteristics, the sulfur atoms may be provided to connect the diradical based molecular wires into the close proximity of the gold electrode, so that the molecular wire can electronically couple to the electrode providing an electrode-sulfur—molecular wire-sulfur-electrode tunneling pathway. Therefore if the distance between two electrodes is small, a better transmission should be expected. For our designed systems the distances between two leads (i.e. between the sulfur atoms) are given in Table 5.12. It is found that, for both odd and even cumulene based diradicals as well as for diradical based on conjugated coupler, with the increase in number of carbon atoms, the distance between two sulfur atoms increases gradually. As a result, there should be a decrease in transmission value with the increase in distance between two electrodes for each series. But the transmission value shows different characteristics for each series. Therefore the two different factors (distance between two leads and the HOMO-LUMO energy gap) affect the transmission. For radical based on conjugated systems two factors counterbalance each other and ultimately a constant transmission value results (in Figure 5.10 (c)).

Table 5.12 Distance between two leads (in Å) (considering the distance between two sulfur atoms).

Systems	Distance between two leads (in Å)	Systems	Distance between two leads(in Å)	Systems	Distance between two leads(in Å)
1(a)	11.33	2(a)	15.53	3(a)	14.82
1(b)	13.32	2(b)	16.97	3(b)	15.72
1(c)	14.52	2(c)	18.56	3(c)	16.59

If the conjugation between the lead and the molecular region is better, higher transmission should be expected. At the same time, greater the distance between S and the rest of the molecular region, lower should be the transmission due to the lower possibility of tunneling of electrons from gold lead to molecular region and *vice versa*. For that reason the distance between S and nearest C has been considered. Though the S-C bond distance for even cumulene based diradicals and diradical based on conjugated systems are equal i.e., 1.68 Å (Figure 5.14 and Figure 5.15), from Figure 5.16 shows that for [3]-cumulene based diradicals as well as for [5]-cumulene based diradicals, the distance between S and C is 1.69Å i.e., remain unaltered, but for [7]-cumulene based diradicals the distance between S and C is 1.74 Å, hence there should be a decrease in transmission, that satisfies the transmission characteristics i.e., a decrease in transmission in [7]- cumulene based diradical systems (in Figure 5.10(a)).

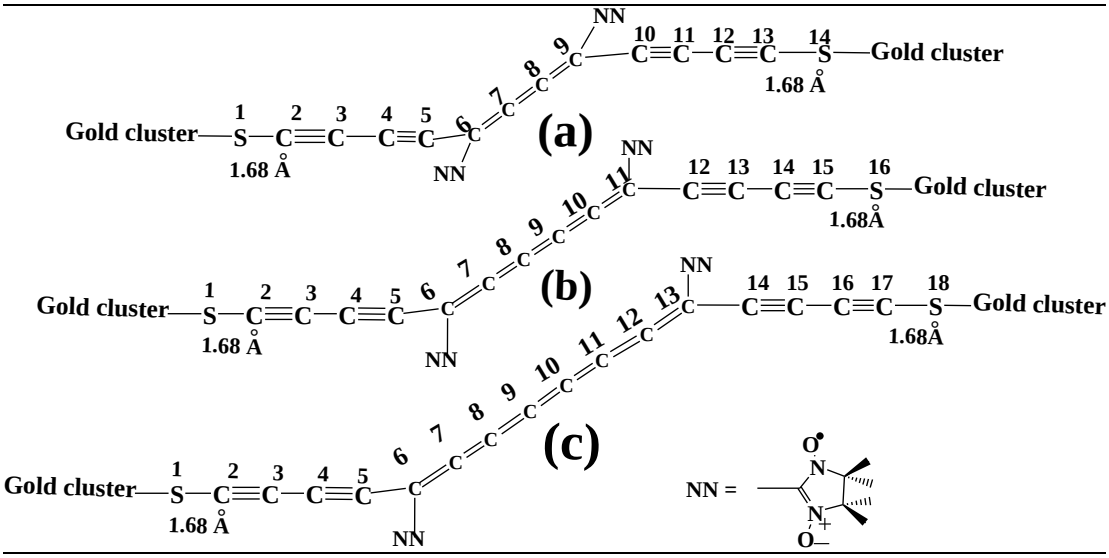

Figure 5.14 Designed even cumulene based molecular wires for the transport calculation.

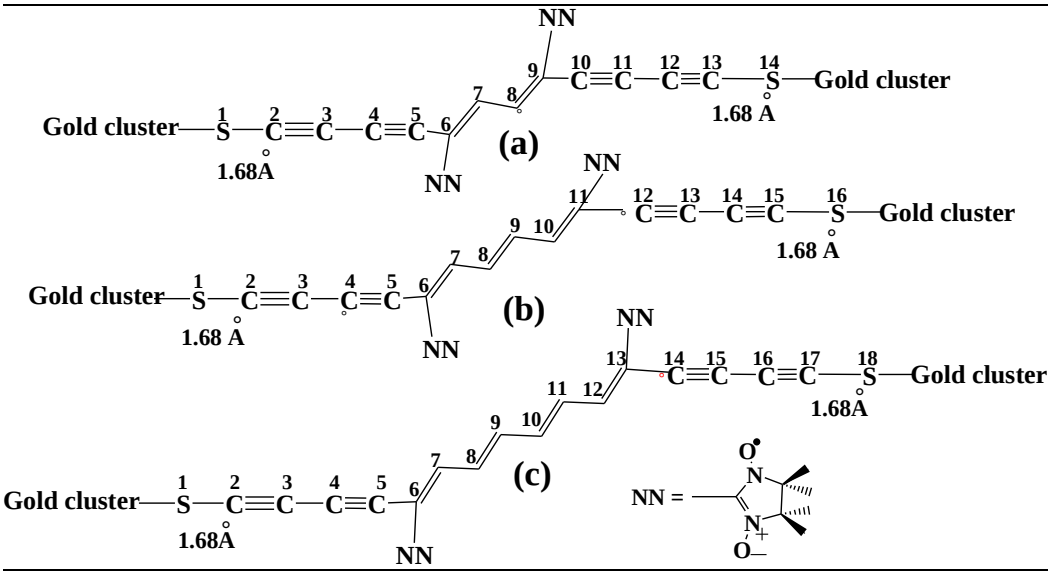

Figure 5.15 Designed conjugated system based molecular wires for the transport calculation.

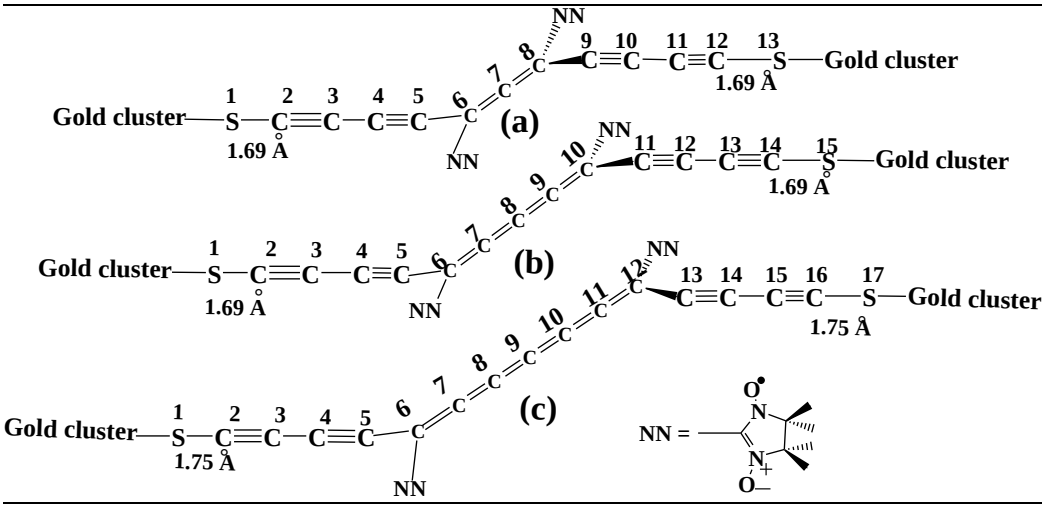

Figure 5.16 Designed odd cumulene based molecular wires for the transport calculation.

(iii) Spin density distribution within the coupler and radical centers

The spin density distributions of the molecular wires attached to the leads are given in Figure 5.17, Figure 5.18, and Figure 5.19.

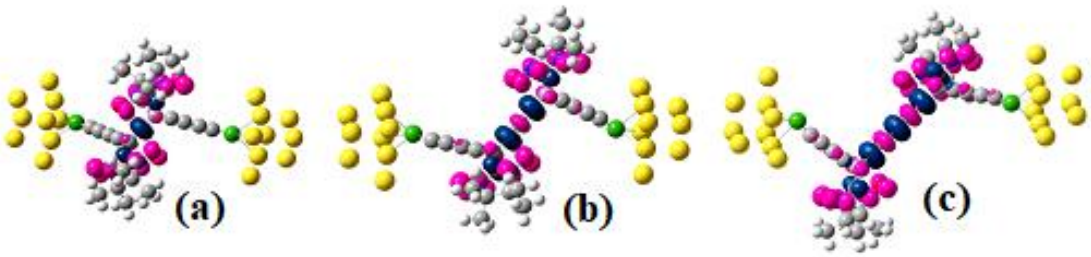

Figure 5.17 Spin polarization pathways within the odd cumulene based molecular wires (iso value 0.004). (a) represents the spin density distribution within allene based molecular wire, (b) represents the spin density distribution within cumulene (containing 5 carbon atoms) based molecular wire, (c) represents the spin density distribution within cumulene (containing 7 carbon atoms) based molecular wire.

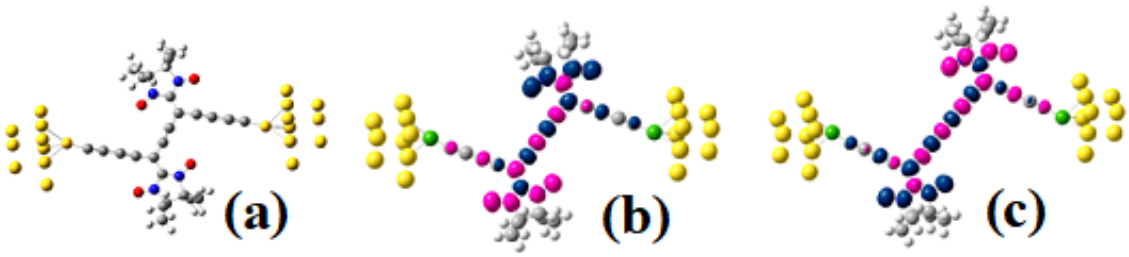

Figure 5.18 Spin polarization pathways within the even cumulene based molecular wires (iso value 0.004). (a) represents the spin density distribution within cumulene (containing 4 carbon atoms) based molecular wire, (b) represents the spin density distribution within cumulene (containing 6 carbon atoms) based molecular wire, (c) represents the spin density distribution within cumulene (containing 8 carbon atoms) based molecular wire.

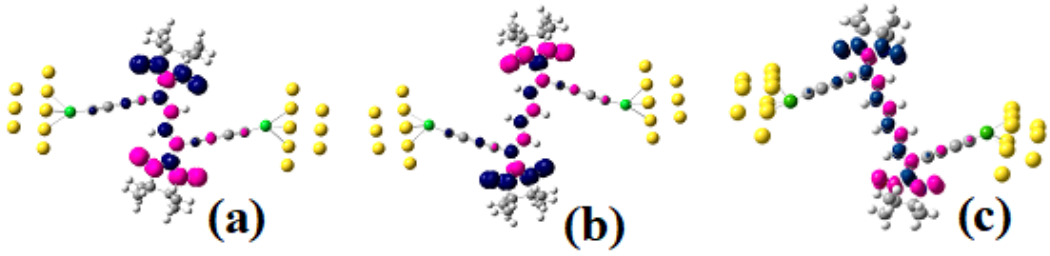

Figure 5.19 Spin polarization pathways within the molecular wires based on conjugated couplers (iso value 0.004). (a) represents the spin density distribution within conjugated systems (containing 4 carbon atoms) based molecular wire, (b) represents the spin density distribution within conjugated systems (containing 6 carbon atoms) based molecular wire, (c) represents the spin density distribution within conjugated systems (containing 8 carbon atoms) based molecular wire.

Figure 5.18 presents some interesting observation that needs further discussion. There seems to be no spin amplitude in the [4]-cumulene fragment in Figure 5.18 (a) but there is substantial amplitude along the chains of length [6]- and [8]-cumulene connector (Figure 5.18 (b) and Figure 5.18 (c)). The spin alternation rule predicts the alpha spin at a radical site will induce beta spin at a neighboring C, alpha at the next and so forth. If two alternating-spin patterns emanating from distinct sites interfere constructively then there will be strong amplitude along the connecting path, and if the interference is destructive there would be no amplitude. As a result of overall destructive interference in Figure 5.18 (a) a diamagnetic situation arises, whereas, in other cases constructive interference occur and high spin amplitude is observed in antiferromagnetic situation (in Figure 5.18(b), Figure 5.18(c)). Such systems can be exploited as logic gates in spintronic applications.[90] Therefore for the system represented in Figure 5.18(a) there occur a spin quenching when such systems are attached to the leads. Thus, an ultimate decrease in transmission in [4]-cumulene based diradicals is observed and a correlation of spin polarization and the transmission characteristics of our designed systems can be intuited.

So, it can be surmised that there are different guiding factors such as the HOMO-LUMO energy gap, distance between two leads as well as the spin polarization that causes the ultimate transmission characteristics in molecular junction transport. The preference of one factor over other causes an increase or decrease in transmission. Finally the origin of all the factors is the unusual π-interaction within the couplers that produce different transmission characteristics of our designed systems.

5.4 Conclusion

To sum up, there is a variation in *J* values for diradicals based on odd cumulene series, diradicals based on even cumulene series and diradicals based on conjugated couplers. It has been found that an existence of distinctive spin polarization pathway in cumulene systems (compared to conjugated systems), distance between two radical centers (that may possibly interrupt the spin polarization pathway) and a planar structure that allows better orbital overlap between π-systems compared to a non planar one, controls the magnetic exchange coupling constant values. Largely speaking, the unusual π-interaction within the coupler is the enlightening factor that controls the magnetic properties of our designed systems. It is also found that the frontier energy splitting, distance between two electrodes and the spin polarization pathways play a major role in determining transmission characteristics of our designed systems.

5.5 References

(1) Kahn, O. Molecular Magnetism. VCH, New York, **1993**.
(2) Lahti, P. M. Magnetic Properties of Organic Materials, Marcel Dekker, New York, **1999**.
(3) Kobayashi, H.; Kobayashi, A.; Cassoux, P. *Chem. Soc. Rev*. **2000**, *29*, 325.
(4) Uji, S.; Shinagawa, H.; Terashima, T.; Yakabe, T.; Terai, Y.; Tokumoto, M.; Kobayashi, A.; Tanaka, H.; Kobayashi, H. *Nature,* **2001**, *410*, 908.
(5) Matsuda, K.; Matsuo, M.; Irie. M. *J. Org. Chem.,* **2001**, *66*, 8799.
(6) Tanifuji, N.; Irie, M.; Matsuda. K. *J. Am. Chem. Soc*.**2005**, *127*, 13344.
(7) Prinz, G. A. *Science*, **1998**, ***282***, 1660.
(8) Emberly, E. G.; Kirczenow, G. *Chem. Phys*. **2002**, *281*, 311.
(9) Wang, F.; Vardeny. Z. V. *J. Mater. Chem.* **2009**, *19*, 1685.
(10) Michelfeit, M.; Schmidt, G.; Geurts, J.; Molenkamp, L. W. *Phys. Status Solidi*, **2008**, *205*, 656.
(11) Nguyen, T. D.; Ehrenfreund, E.; Vardeny, Z. V. *Science,* **2012**, *337*, 204.
(12) Yoo, J. W.; Chen, C. Y.; Jang, H. W.; Bark, C. W.; Prigodin, V. N.; Eom, C. B.; Epstein, A. J. *Nat. Mater.* **2010**, *9*, 638.
(13) Herrmann, C.; Elmisz, J. *Chem. Commun.* **2013**, *49*, 10456.
(14) Eng, M. P.; Albinsson, B. *Angew. Chem., Int. Ed.* **2006**, *45*, 5626.
(15) Wenger. O. S. *Acc. Chem. Res.,* **2011**, *44*, 25.
(16) Nitzan, A.; Ratner, M. A. *Science,* **2003**, *300*, 1384.
(17) Tao, N. J. *Nat. Nanotechnol.,* **2006**, *1*, 173.
(18) Park, B. G.; Wunderlich, J.; Martí, X.; Holý, V.; Kurosaki, Y.; Yamada, M.; Yamamoto, H.; Nishide, A.; Hayakawa, J.; Takahashi, H.; Shick, A. B.; Jungwirth, T. A. *Nat. Mater.,* **2011**, *10*, 347.

(19) Tour, J. M. *Acc. Chem. Res.*, **2000**, *33*, 791.
(20) Winkler, J. R.; Gray, H. B. *J. Am. Chem., Soc*. **2014**, *136*, 2930.
(21) Liu, H.; Wang, N.; Zhao, J.; Guo, Y.; Yin, X.; Boey, F. Y.C.; Zhang, H. *Chem. Phys. Chem*., **2008**, *9*, 1416.
(22) Khoo, K. H.; Chen, Y.; Li, S.; Quek, S. Y. *Phys. Chem. Chem. Phys.*, **2015**, *17*, 77.
(23) Zhao, X. L.; Ando, Y.; Liu, Y.; Jinno, M.; Suzuki, T. *Phys. Rev. Lett.* **2003,** *90*, 187401.
(24) Muramatsu, H.; Hayashi, T.; Kim, Y. A.; Shimamoto, D.; Endo, M.; Terrones, M.; Dresselhaus, M.S. *Nano. Lett*. **2008**, *8*, 237.
(25) Kitaura, R.; Nakanishi, R.; Saito, T.; Yoshikawa, H.; Awaga, K.; Shinohara, H. *Angew. Chem., Int. Ed.*, **2009**, *48*, 8298.
(26) Tobe, Y.; Wakabayashi, T. in *Acetylene Chemistry: Chemistry, Biology, and Material Science* (Eds.: F. Diederich, P. J. Stang, R. R. Tykwinski), Wiley-VCH, Weinheim, **2005**, pp. 387.
(27) Chalifoux, W. A.; Tykwinski, R. R. *Chem. Rec.*, **2006**, *6*, 169.
(28) Shi Shun, A. L. K.; Tykwinski, R. R. *Angew. Chem. Int,. Ed.* **2006**, *45*, 1034.
(29) Raton, B. Polyynes: Synthesis, Properties, and Applications; Cataldo, F. (Eds); Taylor & Francis, **2005.**
(30) Ma, S. *Acc. Chem. Res*. **2009**, *42*, 1679.
(31) Smadja. W. *Chem. Rev*. **1983**, *83*, 263.
(32) Zhang, Y.; Su, Y.; Wang, L.; Kong, E. S.-W.; Chen, X.; Zhang, Y. A. *Nanoscale Research Letters*, **2011**, *6*, 577.
(33) Gu, X.; Kaiser,R. I.; Mebel, A. M. *Chem. Phys. Chem.*, **2008**, *9*, 350.
(34) Weimer, M.; Hieringer, W.; Sala, F. D.; Gçrling, A. *Phys.*, **2005**, *309*, 77.
(35) Skibar, W.; Kopacka, H.; Wurst, K.; Salzmann, C.; Ongania, K. H.; Biani, F. F. D. ; Zanello, P. ; Bildstein, B. *Organometallics*, **2004**, *23*, 1024.
(36) Januszewski, J. A. ; Tykwinski, R.R. *Chem. Soc. Rev.*, **2014**, *43*, 3184.
(37) Januszewski, J. A. ; Wendinger, D.; Methfessel, C. D.; Hampel, F.; Tykwinski, R. R. *Angew. Chem. Int. Ed.*, **2013**, *52*, 1817.
(38) Bhattacharya, D.; Misra, A. *J. Phys. Chem. A*. **2009**, *113*, 5470.
(39) Bhattacharya, D.; Shil, S.; Misra, A.; Klein, D. J. *Theor. Chem. Acc*., **2010**, *127*, 57.
(40) Shil, S.; Sarbadhikary, P.; Misra, A. *RSC Adv*., **2016**, 6, 99467.
(41) Paul, S.; Misra, A. *J. Chem. Theory Comput.* **2012**, *8*, 843.
(42) Paul,S.; Misra, A. *J. Phys. Chem. A.***2010**, *114*, 6641.
(43) Ali, Md. E.; Datta, S. N. *J. Phys. Chem. A.* **2006**, *110*, 2776.
(44) Ko, K. C.; Cho, D.; Lee, J. Y. *J. Phys. Chem. A.* **2013**, *117*, 3561.
(45) Cho, D.; Ko, K.C.; Ikabata, Y.; Wakayama, K.; Yoshikawa, T.; Nakai, H.; Lee, J. Y. *J. Chem. Phys.* **2015**, *142*, 024318.
(46) Nam,Y.; Cho, D.; Lee, J. Y. *J. Phys. Chem. C* **2016**, *120*, 11237.
(47) Cho, D.; Ko, K. C.; Park, H.; Lee, J. Y. *J. Phys. Chem. C* **2015**, *119*, 10109.
(48) Cho, D.; Ko, K. C.; Lee,J. Y. *Int. J. Quant. Chem.* **2016**, *116*, 578.
(49) Ko, K. C.; Cho, D.; Lee, J. Y. *J. Phys. Chem. A* **2012**, *116*, 6837.

(50) Ko, K. C.; Son, S. U.; Lee, S. ; Lee, J. Y. *J. Phys. Chem. B* **2011**, *115*, 8401.
(51) Cho, D.; Ko, K. C.; Lee, J. Y. *J. Phys. Chem. A* **2014**, *118*, 5112.
(52) Ko, K. C.; Park, Y. G.; Cho, D.; Lee, J. Y. *J. Phys. Chem. A* **2014,** *118*, 9596.
(53) Song, M.; Song, X.; Bu, Y. *Chem. Phys. Chem.*, **2017**, *18*, 2487.
(54) Song, M.; Song, X.; Bu, Y. *J. Phys. Chem. C* **2017**, *121*, 21231.
(55) Sarbadhikary, P.; Shil, S.; Panda, A.; Misra, A. *J. Org. Chem,* **2016**, *81*, 5623.
(56) Tamura, M. ; Nakazawa, Y.; Shiomi, D.; Nozawa, K.; Hosokoshi, Y. ; Ishikawa, M.; Takahashi, M. ; Kinosita, M. *Chem. Phys. Lett.*, **1991**, *186***,** 401.
(57) Noodleman, L. *J. Chem. Phys.*, **1981**, *74*, 5737.
(58) Noodleman, L.; Baerends, E. *J. Am. Chem. Soc.*, **1984**, *106*, 2316.
(59) Noodleman, L.; Davidson, E. R. *Chem. Phys.***1986**, *109*, 131.
(60) Noodleman, L.; Peng, C. Y.; Case, D. A.; Mouesca, J. M. *Coord. Chem. Rev.*, **1995**, *144*, 199.
(61) Yamaguchi, K.; Fukui, H.; Fueno, T.*Chem. Lett.* **1986**, *15*, 625.
(62) Yamaguchi, K.; Takahara, Y.; Fueno, T.; Nasu, K. *Jpn. J. Appl. Phys.*, **1987**, *26*, L1362.
(63) Yamaguchi, K.; Jensen, F.; Dorigo, A.; Houk, K. N. *Chem. Phys. Lett.*, **1988**, *149*, 537.
(64) Yamaguchi, K.; Takahara, Y.; Fueno, T.; Houk, K. N. *Theor. Chim. Acta,* **1988**, *73*, 337.
(65) Frisch, M. J.; Trucks, G. W.; Schlegel, H. B.; Scuseria, G. E.; Robb, M. A.; Cheeseman, J. R.; Scalmani, G.; Barone, V.; Mennucci, B.; Petersson, G. A.; Nakatsuji, H.; Caricato, M.; Li, X.; Hratchian, H. P.; Izmaylov, A. F.; Bloino, J.; Zheng, G.; Sonnenberg, J. L.; Hada, M.; Ehara, M.; Toyota, K.; Fukuda, R.; Hasegawa, J.; Ishida, M.; Nakajima, T.; Honda, Y.; Kitao, O.; Nakai, H.; Vreven, T.; Montgomery, J. A., Jr.; Peralta, J. E.; Ogliaro, F.; Bearpark, M.; Heyd, J. J.; Brothers, E.; Kudin, K. N.; Staroverov, V. N.; Kobayashi, R.; Normand, J.; Raghavachari, K.; Rendell, A.; Burant, J. C.; Iyengar, S. S.; Tomasi, J.; Cossi, M.; Rega, N.; Millam, M. J.; Klene, M.; Knox, J. E.; Cross, J. B.; Bakken, V.; Adamo, C.; Jaramillo, J.; Gomperts, R.; Stratmann, R. E.; Yazyev, O.; Austin, A. J.; Cammi, R.; Pomelli, C.; Ochterski, J. W.; Martin, R. L.; Morokuma, K.; Zakrzewski, V. G.; Voth, G. A.; Salvador, P.; Dannenberg, J. J.; Dapprich, S.; Daniels, A. D.; Farkas, Ö.; Foresman, J. B.; Ortiz, J. V.; Cioslowski, J.; Fox, D. J. Gaussian, Inc., Wallingford CT, **2009**.
(66) Büttiker, M.; Imry, Y.; Landauer, R.; Pinhas, S. *Phys. Rev. B,* **1985**, *31*, 6207.
(67) Herrmann, C.; Solomon, G. C.; Subotnik, J. E.; Mujica, V.; Ratner, M. A. *J. Chem. Phys.***2010**, *132*, 024103 (1-17).
(68) Herrmann, C.; Solomon, G. C.; Ratner, M. A. *J. Am. Chem. Soc.*, **2010**, *132*, 3682.
(69) Latif, I. A.; Singh, V. P.; Bhattacharjee, U.; Panda, A.; Datta, S. N. *J. Phys. Chem. A,* **2010**, *114*, 6648–6656.
(70) Herring, C. Magnetism IIB, Direct exchange between well-separated atoms, 5, Eds. G.T. Rado and H. Suhl (**1966**) Academic Press, New York.
(71) Polo, V.; Alberola, A.; Andres, J.; Anthony, J.; Pilkington, M. *Phys. Chem. Chem. Phys*., **2008**, *10*, 857.

(72) Shil, S.; Roy, M.; Misra, A. *RSC Adv*., **2015**, *5*, 105574.
(73) Hermann, C.; Neugebauer, J.; Gladysz, J. A.; Reiher, M. *Inorg. Chem.* **2005**, *44*, 6174.
(74) Prasongkit, J. ; Grigoriev, A.; Wendin, G. ; Ahuja, R. *Phys. Rev. B,***2010**, *81*, 115404.
(75) Kondo, M.; Tada, T. ; Yoshizawa, K. *J. Phys. Chem. A* **2004**, *108*, 9143.
(76) Stuyver, T.; Fias, S. ; Proft, F. De. ; Geerlings, P. *J. Phys. Chem. C*, **2015**, *119*, 26390.
(77) Aravena, D.; Ruiz, E. *J. Am. Chem. Soc*. **2012**, *134*, 777.
(78) Herrmann, C.; Solomon, G. C.; Ratner, M. A. *J. Am. Chem. Soc.,* **2010**, *132*, 3682.
(79) Ashcroft, N. W.; Mermin, N. D. Solid *State Physics*, Holt, Rinehart and Winston, New York, **1976**.
(80) Pauly, F.; Viljas, J. K. ; Cuevas, J. C. ; Schön, G. *Phys. Rev. B,* **2008,** *77*, 155312.
(81) Tour, J. M.; Kozaki, M.; Seminario, J. M. *J. Am. Chem. Soc.,* **1998**,*120*, 8486.
(82) Modelli, A.; Venuti, M.; Scagnolari, F.; Contento, M.; Jones, D. *J. Phys. Chem. A,* **2001**,*105*, 219.
(83) Distefano, G.; Jones, D. ; Guerra, M. ; Favaretto, L. ; Modelli, A. ; Mengoli, G. *J. Phys. Chem.* **1991**, *95*, 9746.
(84) Colle, M. D.; Cova, C.; Distefano, G. ; Jones, D. ; Modelli, A. ; Comisso, N. *J. Phys. Chem. A.* **1999**,*103*, 2828.
(85) Brédas, J. L. ; Thémans, B.; Fripiat, J. G. ; André, J. M. ; Chance, R. R. *Phys. Rev. B,* **1984**,*29*, 6761.
(86) Schlicke, H.; Herrmann, C. *Chem. Phys. Chem.,* **2014**, *15*, 4011.
(87) Proppe, J.; Herrman, C. *J. Comput. Chem.* **2015**, *36*, 201.
(88) Choi, Y. C. ; Kim, W. Y. ; Park, K. S. ; Tarakeshwar, P.; Kim, K. S. ; Kim, T. S. ; Lee, J. Y. *Chem. Phys.*, **2005**, *122*, 094706.
(89) Hermann, C.; Neugebauer, J.; Gladysz, J. A.; Reiher. M. *Inorg. Chem.* **2005**, *44*, 6174.
(90) Chumak, A. V. ; Vasyuchka, V. I. ; Serga, A. A. ; Hillebrands, B. *Nat. Phys.* **2015**, *11*,453.